EPJ Web of Conferences **235**, 01003 (2020) https://doi.org/10.1051/epjconf/202023501003
ISMD 2019

Two-particle correlations on transverse momentum: an untapped resource for studying relativistic heavy-ion collision dynamics

Robert L. Ray[1,⋆] and *Alexander M.* Jentsch[2,⋆⋆]

[1] *Department of Physics, The University of Texas at Austin, Austin, Texas 78712 USA*
[2] *Brookhaven National Laboratory, Upton, New York 11973 USA*

Abstract. Two-particle correlation projections onto two-dimensional transverse momentum coordinates (p_{t1}, p_{t2}) allow access to properties of the relativistic heavy-ion collision system which are complementary to that studied using angular correlations. Examples include the degree of thermal equilibration and the variance of dynamical fluctuations in hard-scattering processes. Results for minimum-bias Au + Au collisions at $\sqrt{s_{NN}} = 200$ GeV are presented, with the structures described by two phenomenological models. The correlations structures and extracted physical quantities are then compared to theoretical predictions. Conclusions from these comparisons regarding global equilibration, fluctuations in soft and semi-hard QCD processes, and the effects of the hot, dense collision medium are presented.

1 Introduction

Two-particle correlation measurements in high-energy, heavy-ion collisions provide access to partonic and hadronic dynamics occurring throughout the spatio-temporal evolution of the hot, dense matter produced in the collisions. In general, these correlations depend on six independent coordinates. However, for most applications only four are relevant, e.g. the relative pseudorapidity and azimuthal angle, $\Delta\eta$ and $\Delta\phi$, and the two-particle transverse momentum coordinates, p_{t1} and p_{t2}. Measurements of correlation distributions on $(\Delta\eta, \Delta\phi)$ are ubiquitous in the heavy-ion literature. Much less attention however, has been given to correlation distributions on transverse momentum. The latter type of measurements have been reported by the NA49 [1, 2], CERES [3], and STAR [4–6] Collaborations. Here, we discuss the features of the nonidentified, two-particle correlation distributions projected on (p_{t1}, p_{t2}) and compare preliminary results with phenomenology and theoretical predictions. Examples of the properties of the heavy-ion collision system which can be deduced by analyzing these correlations are presented and discussed.

2 Analysis method

In Ref. [7] it was shown how to relate two-particle correlation distributions on transverse momentum coordinates to several of the mean-p_t fluctuation quantities in the literature. In the present analysis the

⋆e-mail: ray@physics.utexas.edu
⋆⋆e-mail: alexmichaeljentsch@gmail.com

correlation definition derived from the mean-p_t fluctuation quantity $\Delta\sigma^2_{p_t;n}$, developed and used by the STAR Collaboration [8], was used. The resulting correlation quantity eliminates the statistical bias caused by multiplicity variation within centrality bins. The bias-corrected, event-averaged number of same-event (se) particle pairs and mixed-event (me) pairs, for arbitrary 2D transverse momentum bin k, l, are given by [7]

$$\rho_{\mathrm{se,kl}} = \frac{1}{\epsilon}\sum_{j=1}^{\epsilon}(\bar{N}/n_j)n^{\mathrm{se}}_{j,kl} \tag{1}$$

$$\rho_{\mathrm{me,kl}} = \frac{\bar{N}-1}{\bar{N}\epsilon_{\mathrm{mix}}}\sum_{j\neq j'} n_{jk}n_{j'l}, \tag{2}$$

where all charged particle pairs are included, ϵ is the number of collision events in the centrality or multiplicity bin, and index j denotes a specific event. In Eq. (2) indices j and j' denote arbitrary pairs of mixed-events where ϵ_{mix} is the number of mixed-event permutations included in the multiplicity bin. Also in Eq. (1) $n^{\mathrm{se}}_{j,kl}$ is the number of particle pairs from event j in bin k, l. In Eq. (2) n_{jk} is the number of particles in event j and transverse momentum bin k. Quantity $\bar{N}$ is the mean multiplicity within the acceptance defined by $p_t > 0.15$ GeV/c, $|\eta| < 1$ and full 2π in azimuth corresponding to that of the main tracking detector in the STAR experiment [9].

The per-pair correlation quantity is given by

$$\frac{\Delta\rho_{kl}}{\rho_{\mathrm{me,kl}}} = \frac{\rho_{\mathrm{se,kl}} - \rho_{\mathrm{me,kl}}}{\rho_{\mathrm{me,kl}}}. \tag{3}$$

Multiplication by a pre-factor, defined in Ref. [10], gives a per final-state particle correlation measure which aligns with standard, normalized covariance measures [11] and which, for example, facilitates binary scaling tests. The prefactor is constructed from Levy-model fits to the measured single-particle p_t spectra. Here, we are interested in testing the centrality dependence of the correlation structures with respect to binary scaling. To facilitate this specific test the prefactor will also include an estimate of the soft-process p_t spectrum. The prefactor is given in Ref. [10]; the final correlation quantity is written for brevity as $\Delta\rho/\sqrt{\rho_{\mathrm{soft}}}$. In order to facilitate studies of jet fragment contributions to the correlation structures [12] the correlations are presented on transverse momentum space variable y_t, the *transverse rapidity*, where $y_t = \log[(p_t + m_t)/m_0]$, $m_t = \sqrt{p_t^2 + m_0^2}$ is the transverse mass, and parameter m_0 (pion mass) regulates the divergence as $p_t \to 0$.

Preliminary data from the STAR Collaboration were presented in Refs. [13, 14] for minimum-bias Au+Au collisions at $\sqrt{s_{NN}} = 200$ GeV. These preliminary measurements included all charged-particle pairs but required the relative azimuth of the pairs to be greater than $\pi/2$, i.e. away-side (AS) pairs. Those data were fitted with analytic functions and assigned statistical errors as described in Refs. [10, 14]. The resulting *pseudodata* will be compared to predictions and described with phenomenological models in the following sections.

3 Theoretical predictions

Predictions of HIJING [15] and EPOS [16] are compared with pseudodata for selected centrality bins in figure 1. Both models predict the overall saddle-shape and the peak near $(y_{t1}, y_{t2}) = (3, 3)$ observed in the pseudodata. HIJING combines the LUND [17] model of longitudinal, color-string fragmentation plus PYTHIA [18] which describes semi-hard and hard-scattering jets. In its simplest application HIJING provides a null hypothesis in which heavy-ion collisions are assumed to be a superposition

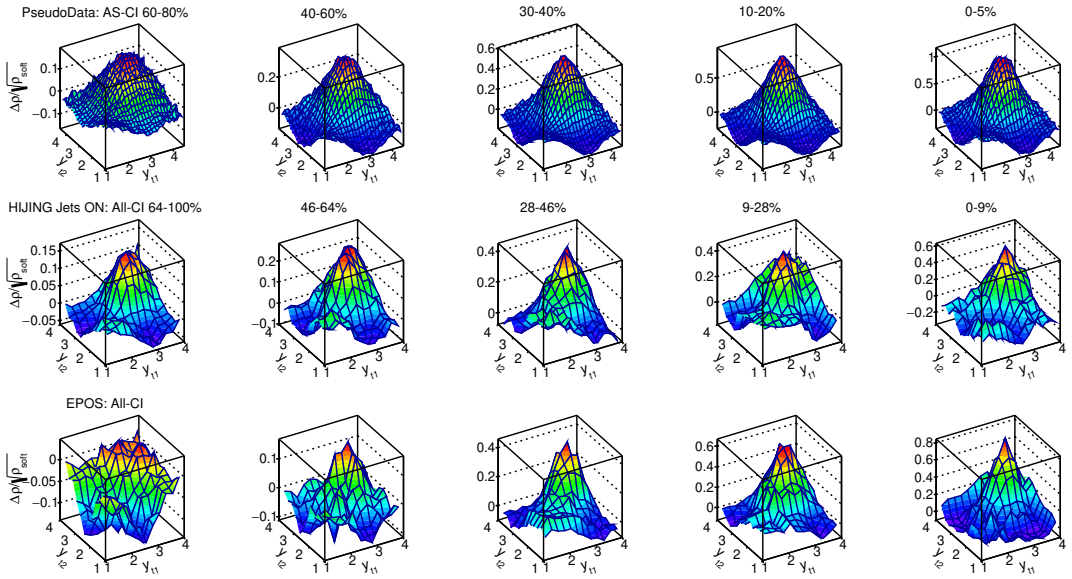

Figure 1. Theoretical model predictions compared with correlation pseudodata $\Delta\rho/\sqrt{\rho_{\rm soft}}$ on coordinates (y_{t1}, y_{t2}) for Au+Au collisions at $\sqrt{s_{NN}}$ = 200 GeV using all charged particle pairs (charge-independent, CI) and relative azimuthal angles greater than $\pi/2$. Pseudodata are shown in the upper row of panels for centrality cross section fractions 60-80%, 40-60%, 30-40%, 10-20% and 0-5% from left-to-right, respectively. The next two rows show, respectively, HIJING model predictions for 200 GeV Au+Au collisions with jets-on, and EPOS predictions. Centralities for the HIJING and EPOS predictions are shown in each row from left-to-right for the coarser cross section fractions 64-100%, 46-64%, 28-46%, 9-28% and 0-9%, respectively.

of independent nucleon + nucleon collisions. In EPOS, fluctuating initial conditions are described in a multiple scattering framework using soft and hard Pomerons. The collision volume is separated into "core" and "corona" domains based on the local energy density and transverse momentum of the interacting partons. Evolution of the core is described using (3+1)D viscous hydrodynamics until the hadronization stage, after which UrQMD [19] describes the final-stage hadronic re-scattering and reactions.

For the HIJING predictions the correlation peak near $(y_{t1}, y_{t2}) = (3, 3)$ increases monotonically with centrality, in general agreement with the trend of the pseudodata. The predicted peak amplitudes for the three more-peripheral bins agree well with the pseudodata, but the predictions are smaller than the pseudodata for the two more-central bins. This result may indicate that the event-wise fluctuation mechanisms in HIJING are realistic for peripheral collisions, with respect to this type of correlation, but fail to describe the most-central correlations. HIJING predictions, without jets included (not shown), completely fail to achieve the observed amplitudes of the (3,3) correlation peak.

The EPOS predictions include both the saddle-shape and a strong (3,3) peak. Except for the 64-100% bin, the peak amplitudes monotonically increase with centrality similar to the pseudodata. The EPOS predicted peak amplitudes for the more-central collisions are in general agreement with the pseudodata. In the two more-peripheral bins the EPOS predicted peak amplitudes are much smaller than either the HIJING jets-on predictions or the pseudodata. The EPOS prediction for the most-peripheral bin is quite dissimilar from the pseudodata. These results suggest that for peripheral collisions the hard-

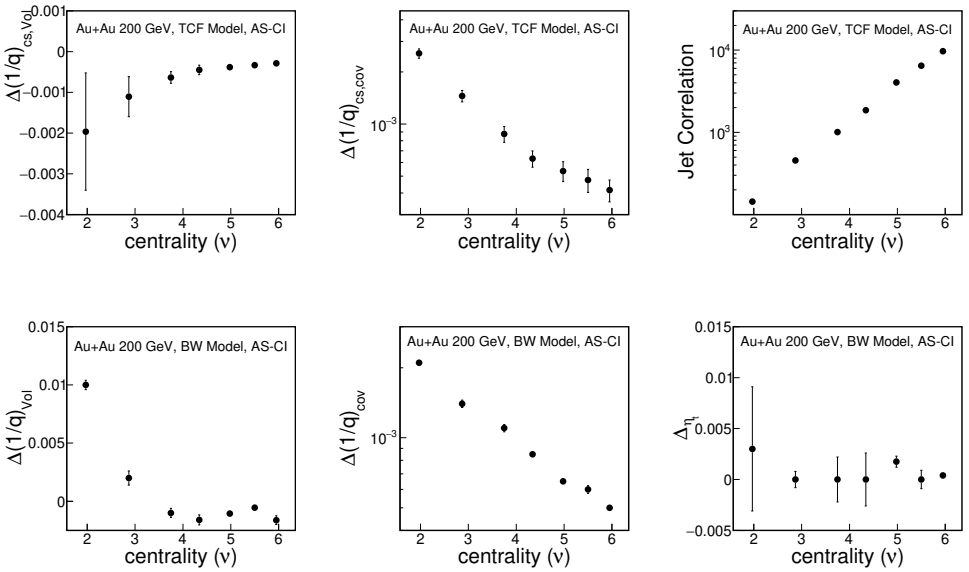

Figure 2. (Upper row): TCF model fit parameters $\Delta(1/q)_{\mathrm{cs,Vol}}$, $\Delta(1/q)_{\mathrm{cs,cov}}$ and jet correlation (covariance) quantity from left-to-right, respectively, as a function of collision centrality measure $\nu = \mathrm{N_{bin}}/(\mathrm{N_{part}}/2)$, where $\mathrm{N_{part}}$ is the number of participating nucleons. (Lower row): Blast-wave fit parameters $\Delta(1/q)_{\mathrm{Vol}}$, $\Delta(1/q)_{\mathrm{cov}}$ and Δ_{η_t} from left-to-right as a function of collision centrality.

scattering contribution is under-estimated by EPOS, while for the more-central collisions, the strong medium-interactions in the model are capable of generating realistic charge-independent correlations.

4 Phenomenology

In order to facilitate the interpretation of these new correlation structures and to offer insight into the possible deficiencies in theoretical approaches, two phenomenological models were developed in Ref. [10]. One is based on the two-component multiplicity production model of Kharzeev, Nardi and Levin [20] and the other is based on the blast-wave [21]. In both models, key elements which determine the particle distributions, e.g. jet energies or freeze-out temperatures, are allowed to fluctuate. All details of the models are given in Ref. [10].

The two-component fragmentation (TCF) model includes color-strings (color flux tubes) and minijets (i.e. jets with no artificial lower energy cut-off). Color-string fragmentation is assumed to produce a Maxwell-Boltzmann p_t distribution with slope parameter β_{cs}. The semi-hard scattering, minijet production is described as the convolution integral of the product of a universal jet fragment distribution [12] times a QCD power-law probability distribution, including a soft-QCD cut-off. Correlations among the final-state particles are generated via correlated β_{cs} values between pairs of particles within a collision event and via correlated minijet energies. The correlation pseudodata were fit by adjusting the overall width and covariance of the two-particle $(\beta_{\mathrm{cs}_1}, \beta_{\mathrm{cs}_2})$ probability distribution, the variance of the event-wise fluctuating semi-hard scattering multiplicity, and the covariance strength of the two-particle, minijet energy distribution. Three of the fit parameters are shown in the upper row of panels

in figure 2 where $\Delta(1/q)_{\rm cs,Vol} = (1/2)(\sigma^2_{\beta_\Sigma} + \sigma^2_{\beta_\Delta} - 2\sigma^2_\beta)/\bar{\beta}^2$ and $\Delta(1/q)_{\rm cs,cov} = (1/2)(\sigma^2_{\beta_\Sigma} - \sigma^2_{\beta_\Delta})/\bar{\beta}^2$. In these definitions σ^2_β is the variance of the fluctuating, single-particle color-string slope parameters whose mean is $\bar{\beta}$. Parameters $\sigma^2_{\beta_{\Sigma,\Delta}}$ are the variances of the 2D $(\beta_{\rm cs_1}, \beta_{\rm cs_2})$ distribution along the $\beta_{\Sigma,\Delta} = \beta_{\rm cs_1} \pm \beta_{\rm cs_2}$ directions.

The major features and centrality trends of the data are well-described. The soft-component contributions and the semi-hard scattering multiplicity variance mainly affect the saddle-shape and its amplitude, while the covariance of the two-particle jet energy distribution mainly affects the (3,3) peak amplitude. The centrality dependence of the latter two, semi-hard scattering quantities were compared with binary collision ($N_{\rm bin}$) scaling. The trend of the semi-hard scattering variance is approximately $\sigma^2_{\rm hard} = (0.213 \pm 0.092)N_{\rm bin}^{1.156\pm0.071}$ and $\sigma^2_{\rm hard} = (0.66 \pm 0.31)\bar{N}_{\rm hard}^{1.12\pm0.09}$ where $\bar{N}_{\rm hard}$ is the semi-hard component mean multiplicity. The latter tests the Poisson limit for fluctuations in the semi-hard component. This variance approximately follows binary scaling and approaches the Poisson limit for more-central collisions; a validation of the TCF approach since this variance is expected to be approximately Poisson. The jet covariance scales as $(0.390 \pm 0.085)N_{\rm bin}^{1.451\pm0.035}$ which exceeds binary scaling, indicating the presence of significant interactions within the medium.

The blast-wave (BW) model describes particle emission from an expanding, hydrodynamic-like source with freeze-out temperature $(1/\beta)$ and transverse flow velocity assuming a Maxwell-Boltzmann source distribution [21]. In the model the freeze-out temperature is allowed to fluctuate both locally and globally from event-to-event as described by a two-particle (β_1, β_2) probability distribution analogous to the preceding 2D distribution for color-strings. The transverse flow velocity, or the corresponding rapidity, is similarly allowed to fluctuate and is parametrized by a peaked, two-particle probability distribution. The correlation data were fit by freely adjusting the overall width and variance of the (β_1, β_2) distribution and the co-variance of the transverse flow rapidity distribution. The fit parameters are shown in the lower row of panels in figure 2 where $\Delta(1/q)_{\rm Vol}$ and $\Delta(1/q)_{\rm cov}$ are defined in the same way as the corresponding TCF parameters, and Δ_{η_t} controls the covariance of the two-particle transverse flow rapidity. The correlation pseudodata are well described where the required, relative changes in the overall width and covariance of the (β_1, β_2) distribution are only of order 10^{-3}, and the covariance in the transverse flow is consistent with zero, i.e. no evidence of correlated transverse flow. The two-particle inverse temperature distribution required to fit the correlation pseudodata is strongly inconsistent with an ensemble of globally equilibrated collisions. The latter would be characterized with maximum, relative covariance.

The HIJING and EPOS predictions were also fit with the TCF and BW phenomenologies, to gain insight into those aspects of the theoretical models which might be deficient. Based on comparisons of the fits to the pseudodata and to the theoretical models, we find that EPOS collisions may be too hot, and for peripheral collisions may either be under-estimating hard-scattering processes or over-estimating the degree of dissipation in the medium (core). Similarly, while HIJING predictions, with jets included, appear reasonable for peripheral collisions, the color-string fluctuations are, in general, not sufficiently correlated, and the jet-like correlations for more-central collisions produce only about half the required amplitude.

5 Conclusions

Analysis of two-particle, pair-number correlation distributions on 2D transverse momentum, or transverse rapidity, provides access to additional properties of the relativistic heavy-ion collision system. These include studies of the degree of thermal equilibration within the hydrodynamic picture, or the variance in hard-scattering processes within the fragmentation approach. In combination with 2D angular correlations, these relatively under-appreciated correlation measurements provide significant, new constraints on theoretical models. Phenomenology, as shown here, helps bridge the gap

between data and theory by enhancing the interpretive value of these measurements and suggesting what upgrades may be needed in the theoretical approaches. A significant quantity of new correlation measurements on transverse rapidity are being prepared by the STAR Collaboration for publication in the near future.

Acknowledgements

The authors would like to thank Professor Thomas Trainor of the Univ. of Washington for many informative discussions relevant to this work and Professor Rainer Fries of Texas A&M University for discussions related to the blast-wave model. This research was supported in part by the Office of Science of the U. S. Department of Energy under Grants No. DE-FG02-94ER40845 and No. DE-SC0013391.

References

[1] J. G. Reid, Nucl. Phys. A **698**, 611c (2002).
[2] S. V. Afanasiev *et al.* (NA49 Collaboration), Nucl. Phys. A **715**, 55c (2003); T. Anticic *et al.* (NA49 Collaboration), Phys. Rev. C **70**, 034902 (2004).
[3] D. Adamová *et al.* (CERES Collaboration), Nucl. Phys. A **811**, 179 (2008).
[4] J. G. Reid, Ph.D. thesis, University of Washington, 2002 (unpublished); arXiv:nucl-ex/0302001.
[5] J. Adams *et al.* (STAR Collaboration), J. Phys. G: Nucl. Part. Phys. **34**, 799 (2007).
[6] T. A. Trainor and D. J. Prindle, Phys. Rev. D **93**, 014031 (2016).
[7] R. L. Ray and P. Bhattarai, Phys. Rev. C **94**, 064902 (2016).
[8] J. Adams *et al.* (STAR Collaboration), Phys. Rev. C **71**, 064906 (2005).
[9] M. Anderson *et al.*, Nucl. Istrum. Meth. Phys. Research A **499**, 659 (2003).
[10] R. L. Ray and A. Jentsch, Phys. Rev. C **99**, 024911 (2019).
[11] J. L. Rodgers and W. A. Nicewander, Am. Stat. **42**, 59 (1988); B. S. Everitt and A. Skrondal, *The Cambridge Dictionary of Statistics*, 4th ed. (Cambridge Univ. Press, Cambridge, 2010), p. 107.
[12] T. A. Trainor, Phys. Rev. C **80**, 044901 (2009); T. A. Trainor and D. T. Kettler, Phys. Rev. D **74**, 034012 (2006).
[13] E. W. Oldag (STAR Collaboration), J. Phys.: Conf. Ser. **446**, 012023 (2013).
[14] E. W. Oldag, Ph.D. thesis, The University of Texas at Austin, 2013 (unpublished), `https://drupal.star.bnl.gov/ STAR/files/oldag_dissertation_20132.pdf`.
[15] X.-N. Wang, M. Gyulassy, Phys. Rev. D **44**, 3501 (1991).
[16] K. Werner, Nucl. Phys. B (Proc. Suppl.) **175-176**, 81 (2008).
[17] B. Andersson, G. Gustafson, G. Ingelman and T. Sjöstrand, Phys. Rep. **97**, 31 (1983).
[18] T. Sjöstrand and M. van Zijl, Phys. Rev. D **36**, 2019 (1987).
[19] H. Sorge, H. Stöcker, W. Greiner, Nucl. Phys. A **498**, 567 (1989); Ann. Phys. (N.Y.) **192**, 266 (1989).
[20] D. Kharzeev and M. Nardi, Phys. Lett. B **507**, 121 (2001); D. Kharzeev, E. Levin and M. Nardi, Nucl. Phys. A **730**, 448 (2004).
[21] E. Schnedermann, J. Sollfrank, U. Heinz, Phys. Rev. C **48**, 2462 (1993).